Bioprocess Biosyst Eng (2013) 36:499–514
DOI 10.1007/s00449-012-0806-1

ORIGINAL PAPER

Biological nitrogen and phosphorus removal in membrane bioreactors: model development and parameter estimation

Alida Cosenza · Giorgio Mannina · Marc B. Neumann · Gaspare Viviani · Peter A. Vanrolleghem

Received: 19 April 2012 / Accepted: 3 August 2012 / Published online: 26 September 2012

Abstract Membrane bioreactors (MBR) are being increasingly used for wastewater treatment. Mathematical modeling of MBR systems plays a key role in order to better explain their characteristics. Several MBR models have been presented in the literature focusing on different aspects: biological models, models which include soluble microbial products (SMP), physical models able to describe the membrane fouling and integrated models which couple the SMP models with the physical models. However, only a few integrated models have been developed which take into account the relationships between membrane fouling and biological processes. With respect to biological phosphorus removal in MBR systems, due to the complexity of the process, practical use of the models is still limited. There is a vast knowledge (and consequently vast amount of data) on nutrient removal for conventional-activated sludge systems but only limited information on phosphorus removal for MBRs. Calibration of these complex integrated models still remains the main bottleneck to their employment. The paper presents an integrated mathematical model able to simultaneously describe biological phosphorus removal, SMP formation/degradation and physical processes which also include the removal of organic matter. The model has been calibrated with data collected in a UCT-MBR pilot plant, located at the Palermo wastewater treatment plant, applying a modified version of a recently developed calibration protocol. The calibrated model provides acceptable correspondence with experimental data and can be considered a useful tool for MBR design and operation.

Keywords ASM2d-SMP · MBR modelling · Membrane fouling · Model calibration · Nitrogen and phosphorus removal

A. Cosenza (✉) · G. Mannina · G. Viviani
Dipartimento di Ingegneria Civile, Ambientale, Aerospaziale, dei Materiali Università di Palermo Viale delle Scienze, 90128 Palermo, Italy
e-mail: alida.cosenza@unipa.it

G. Mannina
e-mail: giorgio.mannina@unipa.it

G. Viviani
e-mail: gaspare.viviani@unipa.it

M. B. Neumann · P. A. Vanrolleghem
modelEAU, Département de génie civil et de génie des eaux, Université Laval, 1065 av. de la Médecine, Québec, QC G1V 0A6, Canada
e-mail: Marc.Neumann@gci.ulaval.ca

P. A. Vanrolleghem
e-mail: Peter.Vanrolleghem@gci.ulaval.ca

Introduction

In the last decade, the use of membrane bioreactor (MBR) technology, for municipal as well as industrial wastewater, has increased significantly. Thanks to its technological advantages and the decreasing cost of membranes [1, 2]. At the same time, the need to improve the MBR process understanding, design and operation has grown. The peculiarities of MBR systems such as the solid–liquid separation, the high suspended solids concentration and the high sludge retention times (SRT) induce vast differences in the sludge properties and dynamic behavior of MBR systems compared to the well-known conventional-activated sludge systems (CASs) [3, 4]. However, some peculiarities of MBR systems still remain poorly understood. For example, controversial literature exists regarding the interactions that occur among factors affecting the

membrane fouling: membrane materials, biomass characteristics, feed-water characteristics and operating conditions [5–7].

In the context of "*MBR knowledge upgrading*" mathematical modeling has undoubtedly played an important role. Several MBR models have been presented in the literature in order to explain the peculiarities of MBRs. In particular, as discussed by [8], the activated sludge models (ASMs), originally developed for CAS systems, have been applied in their original form or adapted in order to simulate the bioprocesses occurring in MBR systems (among others, Jiang et al. [9]; Spérandio and Espinosa [10]; Mannina et al. [11]). The main adaptation of ASM models has been the inclusion of a soluble microbial products (SMPs)—submodel leading to the so-called "hybrid models". Indeed, many authors have demonstrated that the content of extracellular polymeric substances (EPSs) that may be closely bound with cells (EPS bound), weakly bound with cells or dissolved into the solution (EPS soluble or SMP) have a significant influence on membrane fouling, reducing membrane permeability (among others Ahmed et al. [12]). Therefore, a successful prediction of SMP may provide useful information about membrane fouling. Recently, Jiang et al. [9] proposed a hybrid version of ASM2d in which substrate utilization and biomass associated products (S_{UAP} and S_{BAP}) degradation is described by first-order kinetics introducing only four new parameters (f_{BAP}, $k_{h,BAP}$, f_{UAP} and $k_{h,UAP}$) in order to minimize the model complexity.

Regarding the physical process, the MBR modeling literature gives particular attention to the interaction between physical and biological processes by introducing "integrated" models [13]. The integrated models basically couple the biological model (including the SMPs formation/degradation processes according to the "hybrid" configuration models) with the physical models. Zarragoitia-González et al. [14] proposed an integrated model based on the hybrid model introduced by Lu et al. [15], which has the same not balanced stoichiometry problem and presents a high complexity due to the high number of SMP-related parameters.

On the other hand, among the published integrated models only few models take into account the relationships between the reversible fouling (cake layer) and the biological processes. Among these, the model proposed by Di Bella et al. [16] is able to describe the effect of the cake layer on COD removal according to the deep bed theory [17]. This model has recently been improved by Mannina et al. [18] by introducing the evaluation of the membrane permeability variation (in terms of trans-membrane pressure, TMP) and taking into account the reversible and irreversible contribution to the membrane fouling assessment.

Nevertheless, integrated MBR models able to describe the biological nutrient removal (BNR) processes as well as SMP formation/degradation and physical separation are not yet fully available and have yet to be developed [19, 20]. Specifically as underlined in the overview provided by Fenu et al. [8], the need for further studies on MBR phosphorus removal modeling and on the transport of SMPs through the membrane is required. Moreover, the existing integrated models, which introduce new processes (e.g. SMP formation/degradation and physical processes), variables and parameters, are complex and generally characterized by a large number of parameters. Their intrinsic complexity is characteristic of the problems associated with the calibration of the ASM family: parameter identifiability and over-parameterization. Indeed, default ASM parameter values have to be adjusted to respect the operating conditions of the plant under study, the features of the involved influent and biomass and the biological kinetics [21]. In view of the frequent lack of data, the calibration phase is often very laborious before satisfactory results are obtained. In order to help modelers in this crucial phase, different systematic calibration protocols have been proposed: by STOWA [22], BIOMATH [23, 24], Water Environment Research Foundation [25] and Hochschulgruppe [26]. Recently, Mannina et al. [27] have proposed a calibration procedure which considers a preliminary screening of the most important model parameters, by means of a local sensitivity analysis, and their subsequent calibration according to a step-wise approach. All these calibration protocols and procedures are based on a local screening of the model parameters in which the analysis is performed at a given central point in parameter space [28]. In contrast, by applying global sensitivity analysis (GSA) methods the entire parametric space is analyzed at once [29].

Despite the important efforts deployed to tackle the calibration issue, for now the calibration of ASM model, still remains the weakest link in their application [30]. Thus, default parameter values are often used (above all for biological phosphorus removal modeling) strongly influencing the model response [20].

In order to address the above-mentioned weaknesses in the field of MBR modeling, the paper is focused on several aims. An integrated MBR mathematical model is proposed. The integrated model is able to describe the BNR process, SMP formation/degradation according to Jiang et al. [9] and the influence of the cake layer on the COD removal according to Mannina et al. [18]. The model also takes into account the hydrolysis process of the very slowly hydrolysable compound according to Lubello et al. [31].

The integrated model has been applied for modeling processes occurring in a UCT-MBR pilot plant fed with real wastewater. An intensive sampling campaign has been performed in the pilot plant collecting useful data for model calibration. Due to the fact that the proposed model

resulted to be very complex, involving 19 biological state variables for each plant section and 79 model parameters, the calibration issue has been investigated in-depth. More specifically, the modified version of the calibration protocol first proposed by Mannina et al. [27] has been used for model calibration. In particular, in the modified version of the protocol applied here the traditional local sensitivity analysis has been replaced with a GSA [namely, by the Standardized Regression Coefficients (SRC) method]. All data collected during the pilot plant operation has been used for model calibration.

Model description

The MBR model is divided into two sub-models: a biological and a physical sub-model. It involves 19 biological state variables for each plant section and 79 parameters (kinetic, stoichiometric, physical and fractionation-related). Tables 1 and 2, respectively, summarize the kinetic and stoichiometric parts of the Gujer matrix.

The proposed integrated MBR model couples the ASM2d-SMP model first introduced by Jiang et al. [9] with a physical sub-model derived from, Mannina et al. [11] and Di Bella et al. [16].

The biological sub-model is a modified version of ASM2d [9] and takes into account two new state variables, S_{UAP} and S_{BAP}, and six new processes (anaerobic, aerobic and anoxic hydrolysis of both UAP and BAP). The sum of S_{UAP} and S_{BAP} is equal to the modeled SMP. According to Jiang et al. [9], S_{UAP} and S_{BAP} are both defined to have a size <0.45 μm, to be produced in the reactor and to be biodegradable. Jiang's original ASM2d-SMP Gujer matrix has been modified by adjusting the incoherent stoichiometric coefficients [9]. In particular, the Y_H related to the stoichiometric coefficients of S_O and S_{UAP} for the aerobic growth process of X_{PAO} has been replaced with Y_{PAO}, while Y_H related to the stoichiometric coefficients of S_{UAP} for the growth of X_{AUT} has been replaced with Y_{AUT}. Moreover, the kinetic hydrolysis process of very slowly hydrolysable compounds (X_I) according to Lubello et al. [31] has been introduced (26th process of Table 1).

The assumptions, processes and variables of ASM2d are still valid, except for the process (and related variables) of phosphorus precipitation which has been neglected because no chemical flocculants (metal hydroxide) addition has been considered. For the variables and process descriptions, the reader is referred to the description of ASM2d [32]. As discussed above, the advantage of Jiang's hybrid model is that it introduces only four new parameters. In particular, the S_{BAP} production is described to be proportional to the biomass decay and is characterized by the stoichiometric parameter f_{BAP} (fraction of BAP generated per biomass decayed). The S_{BAP} reduction which is due to aerobic, anoxic and anaerobic hydrolysis processes following first order kinetics is characterized by the hydrolysis rate coefficient for S_{BAP} ($k_{H,BAP}$). The S_{UAP} production and degradation are similarly described by introducing the coefficients f_{UAP} (fraction of UAP generated during biomass decay) and $k_{H,BAP}$.

The total COD (COD_{TOT}), total soluble COD (COD_{SOL}), total phosphorus (TP), total nitrogen (TN) and mixed liquor suspended solid (MLSS) concentration are described as follows, where the coefficients in the Eqs. 1–5 are defined according to ASM2d:

$$COD_{TOT} = S_F + S_A + S_I + S_{UAP} + S_{BAP} + X_I + X_S + X_H + X_{AUT} + X_{PAO} + X_{PHA} \quad (1)$$

$$COD_{SOL} = S_F + S_A + S_I + S_{UAP} + S_{BAP} \quad (2)$$

$$TP = S_{PO_4} + i_{PSF} \cdot S_F + i_{PSI} S_I + i_{PXS} \cdot X_S + i_{PXI} \cdot X_I + i_{PBM} \cdot (X_H + X_{AUT} + X_{PAO}) + X_{PP} \quad (3)$$

$$TN = S_{NO_3} + S_{NH_4} + i_{NSF} \cdot S_F + i_{NSI} S_I + i_{NXS} \cdot X + i_{NXI} \cdot X_I + i_{NBM} \cdot (X_H + X_{AUT} + X_{PAO}) \quad (4)$$

$$MLSS = i_{TSS,XI} \cdot X_I + i_{TSS,XS} \cdot X_S + i_{TSS,BM} \cdot (X_H + X_{AUT} + X_{PAO}) + i_{TSS,XPP} \cdot X_{PP} + i_{TSS,XPHA} X_{PHA} \quad (5)$$

The physical sub-model is derived from an integrated MBR model developed in previous studies [11, 16]. The model describes the cake layer formation during the suction and backwashing phases and the partial COD removal throughout the cake layer, taking into account the reversible fouling of the membrane. In particular, according to the model proposed by Li and Wang [33] and the application proposed by Di Bella et al. [16] and Mannina et al. [18], the rate of sludge attachment and detachment on the membrane surface are modeled continuously throughout the suction and backwashing phase, making it possible to evaluate the solid mass deposited on the membrane surface and the cake layer thickness, $\delta(t)$ at any time (see Di Bella et al. [16], Mannina et al. [18]). Subsequently, by applying the deep-bed theory [17] with the approach of Jang et al. [34], the physical sub-model is able to describe the soluble COD profile across the biological membrane represented by the cake layer [16]. Such a biological membrane is formed by the pool of colloids, solute and particles deposited on the membrane surface. A fraction of particles is retained inside the cake layer which has the function of a biological membrane. Thus, the COD_{TOT} on the cake layers outer surface (which represents the output of the biological model) is reduced across the membrane before the physical filtration. Finally, the model describes the total physical and biological contribution to COD_{TOT} removal which

Table 1 Kinetic process rates for the proposed model

j	Process	Process rate equation ρ_j
1	Aerobic hydrolysis of BAP	$K_{h,BAP}\ [S_{O_2}/(K_{O_2,HYD} + S_{O_2})]\ S_{BAP}X_H$
2	Anoxic hydrolysis of BAP	$K_{h,BAP}\ \eta_{NO_3,HYD}\ [K_{O_2,HYD}/(K_{O_2,HYD} + S_{O_2})]\ [S_{NO_3}/(K_{NO_3,HYD} + S_{NO_3})]\ S_{BAP}X_H$
3	Anaerobic hydrolysis of BAP	$K_{h,BAP}\eta_{fe}\ [K_{O_2,HYD}/(K_{O_2,HYD} + S_{O_2})]\ [K_{NO_3,HYD}/(K_{NO_3,HYD} + S_{NO_3})]\ S_{BAP}X_H$
4	Aerobic hydrolysis of UAP	$K_{h,UAP}\ [S_{O_2}/(K_{O_2,HYD} + S_{O_2})]\ S_{UAP}X_H$
5	Anoxic hydrolysis of UAP	$K_{h,UAP}\ \eta_{NO_3,HYD}\ [K_{O_2,HYD}/(K_{O_2,HYD} + S_{O_2})]\ [S_{NO_3}/(K_{NO_3,HYD} + S_{NO_3})]\ S_{UAP}X_H$
6	Anaerobic hydrolysis of UAP	$K_{h,UAP}\eta_{fe}\ [K_{O_2,HYD}/(K_{O_2,HYD} + S_{O_2})]\ [K_{NO_3,HYD}/(K_{NO_3,HYD} + S_{NO_3})]\ S_{UAP}X_H$
7	Aerobic hydrolysis	$K_h\ [S_{O_2}/(K_{O_2,HYD} + S_{O_2})]\ [(X_S/X_H)/(K_X + (Xs/X_H))]\ X_H$
8	Anoxic hydrolysis	$K_h\ \eta_{NO_3,HYD}\ [K_{O_2,HYD}/(K_{O_2,HYD} + S_{O_2})]\ [S_{NO_3}/(K_{NO_3,HYD} + S_{NO_3})]$ $[(X_S/X_H)/(K_X + (X_S/X_H))]\ X_H$
9	Anaerobic hydrolysis	$K_h\ \eta_{fe}\ [K_{O_2,HYD}/(K_{O_2,HYD} + S_{O_2})]\ [K_{NO_3,HYD}/(K_{NO_3,HYD} + S_{NO_3})]$ $[(X_S/X_H)/(K_X + (X_S/X_H))]\ X_H$
10	Aerobic growth on S_F	$\mu_H\ [S_{O_2}/(K_{O_2,H} + S_{O_2})]\ [S_F/(K_F + S_F)]\ [S_F/(S_F + S_A)]\ [S_{NH_4}/(K_{NH_4,H} + S_{NH_4})]$ $[S_{PO_4}/(K_{P,H} + S_{PO_4})]\ [S_{ALK}/(K_{ALK,H} + S_{ALK})]\ X_H$
11	Aerobic growth on S_A	$\mu_H\ [S_{O_2}/(K_{O_2,H} + S_{O_2})]\ [S_A/(K_{A,H} + S_A)]\ [S_A/(S_F + S_A)]\ [S_{NH_4}/(K_{NH_4,H} + S_{NH_4})]$ $[S_{NH_4}/(K_{P,H} + S_{PO_4})]\ [S_{ALK}/(K_{ALK,H} + S_{ALK})]\ X_H$
12	Anoxic growth on S_F	$\mu_H\ \eta_{NO_3,H}\ [K_{O_2,H}/(K_{O_2,H} + S_{O_2})]\ [S_{NO_3}/(K_{NO_3,H} + S_{NO_3})]\ [S_F/(K_F + S_F)]\ [S_F/(S_F + S_A)]$ $[S_{NH_4}/(K_{NH_4,H} + S_{NH_4})]\ [S_{PO_4}/(K_{P,H} + S_{PO_4})]\ [S_{ALK}/(K_{ALK,H} + S_{ALK})]\ X_H$
13	Anoxic growth on S_A	$\mu_H\ \eta_{NO_3,H}\ [K_{O_2,H}/(K_{O_2,H} + S_{O_2})]\ [S_{NO_3}/(K_{NO_3,H} + S_{NO_3})]\ [S_A/(K_{A,H} + S_A)]\ [S_A/(S_F + S_A)]$ $[S_{NH_4}/(K_{NH_4,H} + S_{NH_4})]\ [S_{PO_4}/K_{P,H} + S_{PO_4})]\ [S_{ALK}/(K_{ALK,H} + S_{ALK})]\ X_H$
14	Fermentation	$q_{fe}\ [K_{O_2,H}/(K_{O_2,H} + S_{O_2})]\ [K_{NO_3,H}/(K_{NO_3,H} + S_{NO_3})]\ [S_F/(K_{fe} + S_F)]$ $[S_{ALK}/(K_{ALK,H} + S_{ALK})]\ X_H$
15	Lysis of X_H	$b_H\ X_H$
16	Storage of X_{PHA}	$q_{PHA}\ [S_A/(K_{A,PAO} + S_A)]\ [S_{ALK}/(K_{ALK,PAO} + S_{ALK})]\ [(X_{PP}/X_{PAO})/(K_{PP} + (X_{PP}/X_{PAO}))]$ X_{PAO}
17	Aerobic storage of X_{PP}	$q_{PP}\ [S_{O_2}/(K_{O_2,PAO} + S_{O_2})]\ [S_{PO_4}/(K_{PS} + S_{PO_4})]\ [S_{ALK}/(K_{ALK,PAO} + S_{ALK})]\ [(X_{PHA}/X_{PAO})/$ $(K_{PHA} + (X_{PHA}/X_{PAO}))]\ [(K_{max} - X_{PP}/X_{PAO})/(K_{IPP} + K_{max} - (X_{PP}/X_{PAO}))]\ X_{PAO}\ q_{PP}$ $\eta_{NO_3,PAO}\ [S_{NO_3}/(K_{NO_3,PAO} + S_{NO_3})]\ [K_{O_2}/(K_{O_2,PAO} + S_{O_2})]\ [S_{PO_4}/(K_{PS} + S_{PO_4})]$
18	Anoxic storage of X_{PP}	$[S_{ALK}/(K_{ALK,PAO} + S_{ALK})]\ [(X_{PHA}/X_{PAO})/(K_{PHA} + (X_{PHA}/X_{PAO}))]$ $[(K_{max} - X_{PP}/X_{PAO})/(K_{IPP} + K_{max} - (X_{PP}/X_{PAO}))]\ X_{PAO}$
19	Aerobic growth of X_{PAO}	$\mu_{PAO}\ [S_{O_2}/(S_{O_2,PAO} + S_{O_2})]\ [S_{NH_4}/(K_{NH_4,PAO} + S_{NH_4})]\ [S_{PO_4}/(K_{P,PAO} + S_{PO_4})]$ $[S_{ALK}/(K_{ALK,PAO} + S_{ALK})]\ [(X_{PHA}/X_{PAo})/(K_{PHA} + (X_{PHA}/X_{PAO}))]\ X_{PAO}$
20	Anoxic growth of X_{PAO}	$\mu_{PAO}\ \eta_{NO_3,PAO}\ [K_{O_2,PAO}/(K_{O_2,PAO} + S_{O_2})]\ [S_{NO_3}/(K_{NO_3,PAO} + S_{NO_3})]\ [S_{NH_4}/$ $(K_{NH_4,PAO} + S_{NH_4})]\ [S_{PO_4}/(K_{P,PAO} + S_{PO_4})]\ [S_{ALK}/(K_{ALK,PAO} + S_{ALK})]$ $[(X_{PHA}/X_{PAO})/(K_{PHA} + (X_{PHA}/X_{PHO}))]\ X_{PAO}$
21	Lysis of X_{PAO}	$b_{PAO}\ X_{PAO}\ [S_{ALK}/(K_{ALK,PAO} + S_{ALK})]$
22	Lysis of X_{PP}	$b_{PP}\ [S_{ALK}/(K_{ALK,PAO} + S_{ALK})]\ [X_{PP}/X_{PAO}]\ X_{PAO}$
23	Lysis of X_{PHA}	$b_{PHA}\ [S_{ALK}/(K_{ALK,PAO} + S_{ALK})]\ [X_{PHA}/X_{PAO}]\ X_{PAO}$
24	Aerobic growth of X_{AUT}	$\mu_{AUT}\ [S_{O_2}/(K_{O_2,AUT} + S_{O_2})]\ [S_{NH_4}/(K_{NH_4,AUT} + S_{NH_4})]\ [S_{PO_4}/(K_{P,AUT} + S_{PO_4})]$ $[S_{ALK}/(K_{ALK,AUT} + S_{ALK})]\ X_{AUT}$
25	Lysis X_{AUT}	$b_{AUT}\ X_{AUT}$
26	Hydrolysis of X_I	$K_i\ X_I$

depends on the fraction of particles removed by the bed (according to the deep bed theory) and on the fraction of particles retained by the physical membrane. The connection between the two sub-models is represented by the MLSS concentration in the MBR reactor.

Data collected during the sampling campaign were used to compose a continuous input series by employing a Fourier series model [27].

Pilot plant and sampling campaign description

The model was applied and calibrated to a UCT-MBR pilot plant (Fig. 1) located at the Acqua dei Corsari (Palermo) wastewater treatment plant (WWTP). The pilot plant consisted of three reactors in series, anaerobic (mean volume 72 L), anoxic (mean volume 165 L) and aerobic (mean volume 327 L), respectively, followed by an aerobic

Table 2 Stoichiometry for the proposed model

Variable	S_{O2}	S_F	S_A	S_{BAP}	S_{UAP}	S_{NH4}	S_{NO3}	S_{PO4}	S_I	S_{ALK}	S_{N2}	X_I	X_S	X_H	X_{PAO}	X_{PP}	X_{PHA}	X_{AUT}	X_{TSS}
Process																			
1		$1-f_{SI}$		-1					f_{SI}										
2		$1-f_{SI}$		-1					f_{SI}										
3		$1-f_{SI}$		-1					f_{SI}										
4		$1-f_{SI}$			-1				f_{SI}										
5		$1-f_{SI}$			-1				f_{SI}										
6		$1-f_{SI}$			-1				f_{SI}										
7		$1-f_{SI}$				$v_{7,NH4}$		$v_{7,PO4}$	f_{SI}	$(1/14)*v_{7,NH4}+(-1.5/31)*v_{7,PO4}$			-1						$-i_{TSS,XS}$
8		$1-f_{SI}$				$v_{8,NH4}$		$v_{8,PO4}$	f_{SI}	$(1/14)*v_{8,NH4}+(-1.5/31)*v_{8,PO4}$			-1						$-i_{TSS,XS}$
9		$1-f_{SI}$				$v_{9,NH4}$		$v_{9,PO4}$	f_{SI}	$(1/14)*v_{9,NH4}+(-1.5/31)*v_{9,PO4}$			-1						$-i_{TSS,XS}$
10	$v_{10,SO2}$	$-1/Y_H$			f_{UAP}/Y_H	$v_{10,NH4}$		$v_{10,PO4}$		$(1/14)*v_{10,NH4}+(-1.5/31)*v_{10,PO4}$				1					$i_{TSS,BM}$
11	$v_{11,SO2}$		$-1/Y_H$		f_{UAP}/Y_H	$-i_{N,BM}$		$-i_{P,BM}$		$(1/14)*v_{11,NH4}+(-1.5/31)*v_{11,PO4}+(-1/64)*v_{11,SA}$				1					$i_{TSS,BM}$
12		$-1/Y_H$			f_{UAP}/Y_H	$v_{12,NH4}$	$v_{12,NOx}$	$v_{12,PO4}$		$(1/14)*v_{12,NH4}+(-1.5/31)*v_{12,PO4}+(-1/14)*v_{12,NOx}$	$v_{12,N2}$			1					$i_{TSS,BM}$
13			$-1/Y_H$		f_{UAP}/Y_H	$-i_{N,BM}$	$v_{13,NOx}$	$-i_{P,BM}$		$(1/14)*v_{13,NH4}+(-1.5/31)*v_{13,PO4}+(-1/14)*v_{13,NOx}+(-1/64)*v_{13,SA}$	$v_{13,N2}$			1					$i_{TSS,BM}$
14		-1	1			$i_{N,SF}$		$i_{P,SF}$		$(1/14)*v_{14,NH4}+(-1.5/31)*v_{14,PO4}+(-1/64)$									
15				f_{BAP}		$v_{15,NH4}$		$v_{15,PO4}$		$(1/14)*v_{15,NH4}+(-1.5/31)*v_{15,PO4}$		f_{XI}	$v_{15,XS}$	-1					$v_{15,TSS}$
16			-1					Y_{PO4}		$(-(-1/64))+(-1.5/31)*Y_{PO4}-(-1/31)*Y_{PO4}$						$-Y_{PO4}$	1		$v_{16,TSS}$
17	$-Y_{PHA}$							-1		$(-(-1.5/31))+(-1/31)$						1	$-Y_{PHA}$		$v_{17,TSS}$
18							$-Y_{PHA}*(1/i_{NOx,N2})$	-1		$(-(-1.5/31))+(-1/14)*v_{18,NOx}+(-1/31)$	$Y_{PHA}*(1/i_{NOx,N2})$					1	$-Y_{PHA}$		$v_{18,TSS}$
19	$v_{19,SO2}$				f_{UAP}/Y_{PAO}	$-i_{N,BM}$		$-i_{P,BM}$		$(1/14)*v_{19,NH4}-i_{P,BM}*(-1.5/31)$					1		$-1/Y_{PAO}$		$v_{19,TSS}$
20					f_{UAP}/Y_{PAO}	$-i_{N,BM}$	$v_{20,NOx}$	$-i_{P,BM}$		$(1/14)*v_{20,NH4}+(-1/14)*v_{20,NOx}-i_{P,BM}*(-1.5/31)$	$v_{20,N2}$				1		$-1/Y_{PAO}$		$v_{20,TSS}$
21				f_{BAP}		$v_{21,NH4}$		$v_{21,PO4}$		$(1/14)*v_{21,NH4}+(-1.5/31)*v_{21,PO4}$		f_{XI}	$v_{21,XS}$		-1				$v_{21,TSS}$

Table 2 continued

Variable	S_{O2}	S_F	S_A	S_{BAP}	S_{UAP}	S_{NH4}	S_{NO3}	S_{PO4}	S_I	S_{ALK}	S_{N2}	X_I	X_S	X_H	X_{PAO}	X_{PP}	X_{PHA}	X_{AUT}	X_{TSS}
22								1		(-(-1.5/31))-(-1/31)						-1			$-i_{TSS,XPP}$
23			1							(-1/64)							-1		$-i_{TSS,XPHA}$
24	-(-(-64/14)-Y_A-f_{UAP}/Y_A				f_{UAP}/Y_A	-$i_{N,BM}$-1/Y_A	1/Y_A	-$i_{P,BM}$		(-$i_{N,BM}$-1/Y_A)*(1/14)+1/Y_A*(-1/14)-$i_{P,BM}$*(-1.5/31)								1	$i_{TSS,BM}$
25				f_{BAP}		$v_{25,NH4}$		$v_{25,PO4}$		(1/14)*$v_{25,NH4}$+(-1.5/31)*$v_{25,PO4}$		f_{XI}	$v_{25,XS}$					-1	$v_{25,TSS}$
26		c_i*(1-$f_{i,I}$)	(1-c_i)*(1-$f_{i,I}$)			$i_{N,Xi}$		$i_{P,XI}$	$f_{i,i}$			-1							

where: $v_{10,SO2} = v_{11,SO2} = -(1-Y_H - f_{UAP})/Y_H$; $v_{19,SO2} = -(1-Y_{PAO}-f_{UAP})/Y_{PAO}$; $v_{7,NH4} = v_{8,NH4} = v_{9,NH4} = -((1-f_{SI})*i_{N,SF}+f_{SI}*i_{N,SI}-i_{N,XS})$; $v_{10,NH4} = v_{12,NH4} = -(-1/Y_H*i_{N,SF}+i_{N,BM})$; $v_{15,NH4} = v_{21,NH4} = v_{25,NH4} = -(f_{XI}*i_{N,XI}+(1-f_{XI})*i_{N,XS}-i_{N,BM})$; $v_{12,NOx} = v_{13,NOx} = -(1-Y_H-f_{UAP})/(i_{NOx,N2}*Y_H)$; $v_{20,NOx} = -(1-Y_{PAO}-f_{UAP})/Y_{PAO}*(1/i_{NOx,N2})$; $v_{7,PO4} = v_{8,PO4} = v_{9,PO4} = -((1-f_{SI})*i_{P,SF}+f_{SI}*i_{P,SI}-i_{P,XS})$; $v_{10,PO4} = v_{12,PO4} = -(-1/Y_H*i_{P,SF}+i_{P,BM})$; $v_{15,PO4} = v_{21,PO4} = v_{25,PO4} = -(i_{P,XI}*f_{XI}+(1-f_{XI})*i_{P,XS}-i_{P,BM})$; $v_{12,N2} = v_{13,N2} = (1-Y_H)/(i_{NOx,N2}*Y_H)$; $v_{20,N2} = (1-Y_{PAO})/Y_{PAO}*(1/i_{NOx,N2})$; $v_{15,XS} = v_{21,XS} = v_{25,XS} = 1-f_{XI}-f_{BAP}$; $v_{15,TSS} = v_{21,TSS} = v_{25,TSS} = f_{XI}*i_{TSS,XI}+(1-f_{XI})*i_{TSS,XS}-i_{TSS,BM}$; $v_{16,TSS} = -Y_{PO4}*i_{TSS,XPP}+i_{TSS,XPHA}$; $v_{17,TSS} = v_{18,TSS} = i_{TSS,XPP}-Y_{PHA}*i_{TSS,XPHA}$; $v_{19,TSS} = v_{20,TSS} = i_{TSS,BM}-1/Y_{PAO}*i_{TSS,XPHA}$

container (mean volume 52 L) where two submerged hollow fiber membrane modules (Zenon Zeeweed, ZW 10) were installed. The presence of the oxygen depletion reactor (ODR) ensures anoxic conditions in the second reactor despite the intensive aeration in the aerobic tank. Each membrane module is characterized by a pore size of 0.04 μm and a nominal surface of 0.93 m^2. The pilot plant was fed with 40 L/h (Q_{FEED}) of municipal wastewater withdrawn by the real WWTP. In this way, it has been possible to reproduce all operational problems connected to the variability of real wastewater. In order to quickly achieve steady state conditions [8], the pilot plant was started up by inoculation with activated sludge to obtain an initial MLSS concentration of 2,900 mg L^{-1}. The permeate was extracted using an ad-hoc permeate extraction pump (for each membrane) by imposing an average flux of 42 L m^{-2} h^{-1} on the membrane surface and a maximum depression (which occurs during the extraction period) of −0.50 bar. The membranes were periodically backwashed (every 9 min for a period of 1 min) by pumping a fraction of the permeate back through the membrane. The membranes were periodically subjected to physical and chemical cleaning. During the physical cleaning, the membranes' surface was periodically flushed with water and cleaned with a sponge to remove the fouling cake layers. Chemical cleaning was conducted by using a solution of 2 g L^{-1} of citric acid in order to reduce the TMP. The plant was operated for 165 days. Until day 76, it was operated with complete sludge retention while after day 76, the sludge was regularly withdrawn, maintaining the sludge age near 37 days. The average MLSS concentrations ranged from 3 to 6.5 g TSS L^{-1} L with an average volatile fraction of 70 % and an average value of the Food/Microorganism ratio (F/M) equal to 0.13 kg COD kg VSS^{-1} day^{-1}. In order to investigate the activity of phosphorus accumulating organisms, during the plant operation, the total phosphorus concentration (P_{TOT}) of the influent was (for specific days) increased by dosing of KH_2PO_4 up to a maximum value of 15.6 mg P L^{-1} (days 119–126 and days 145–165).

Table 3 reports the influent wastewater characteristics related to the entire experimentation period (without the addition of KH_2PO_4). The high maximum value of TKN compared to the NH_4-N demonstrates that for some days of the plant operation the influent wastewater was characterized by high organic nitrogen (higher than the typical values for municipal wastewater). The high organic nitrogen has led to ammonification phenomena producing intense nitrification influencing the denitrification and the phosphorus removal process [4].

During the entire period, the composite influent wastewater (location 0), the grab mixed liquor in each tank (locations 1–4), the mixed liquor in the ODR (location 6)

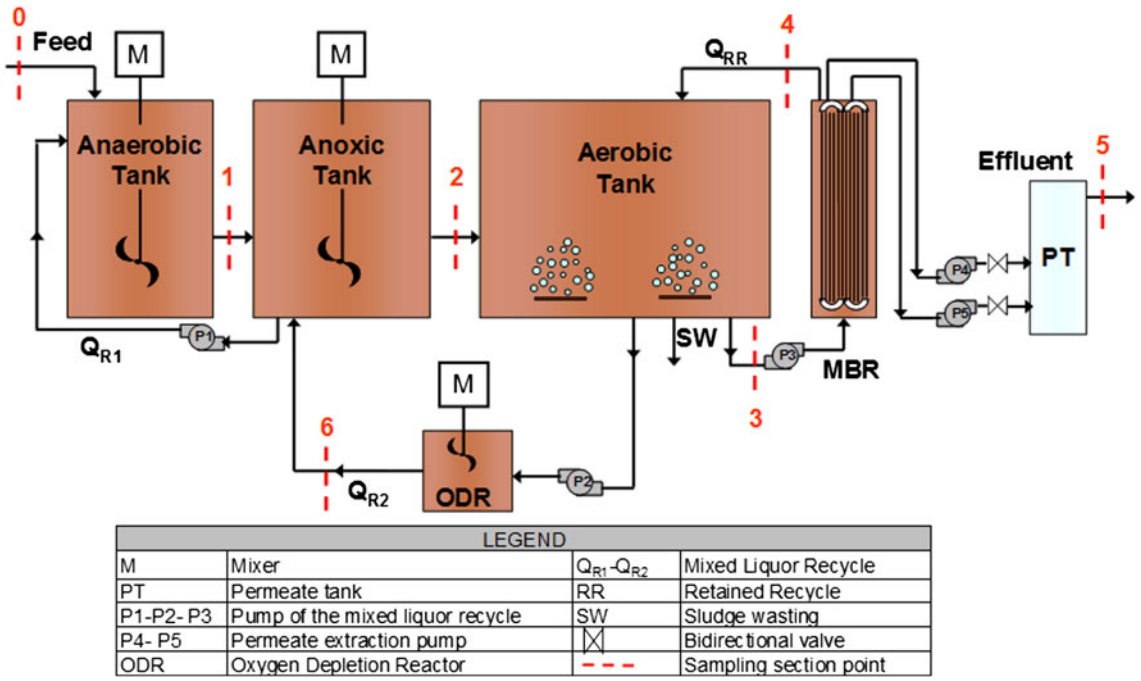

Fig. 1 Schematic overview of the UCT-MBR pilot plant

and the permeate (location 5) were sampled three times per week and analyzed for total and volatile suspended solids (TSS and VSS), total and soluble COD, NH_4-N, NO_2-N, NO_3-N, N_{TOT}, P_{TOT} [35]. Thus, for each analyzed compound in each section about 72 measured data points were obtained. Moreover, daily measurements in each location were conducted for dissolved oxygen (DO), pH and temperature (T) using a handheld Multi-meter 340i (WTW). A physical–chemical characterization of the influent was performed by analyzing COD, NH_4-N, NO_2-N, NO_3-N, N_{TOT} and P_{TOT} from influent grab samples withdrawn at hourly intervals during 24 h. Data collected during the sampling campaign were strongly influenced by unexpected events such as energy interruptions or non-municipal discharges into the municipal sewer system of Palermo [4]. Regarding the plant performance good results were obtained, an average, during the plant operation in terms of COD removal (95 %), nitrification (98 %), denitrification (70 %) and phosphorus removal (60 %). Further details about the pilot plant, sampling campaign and performance can be found in [4].

Table 3 Influent wastewater characteristics

Parameter	Unit	Average	Max	Min
COD_{TOT}	mg L^{-1}	327	525	138
$COD_{TOT,FIL}$	mg L^{-1}	104	283	42
BOD	mg L^{-1}	176	250	90
NH_4-N	mg L^{-1}	16	30	4
NO_x-N	mg L^{-1}	2	11	0
TKN	mg L^{-1}	91	291	12
PO_4-P	mg L^{-1}	1.5	2	0.5
P_{TOT}	mg L^{-1}	4	13	2
TSS	mg L^{-1}	282	736	109
VSS	mg L^{-1}	177	404	60
COD/N/P	–	100/28.5/1.16		
T	°C	21	26	18.9
pH	–	7.6	8.4	7

Sensitivity analysis and model calibration

The first phase of the protocol proposed by Mannina et al. [27] performs the parameter subsets selection by means of sensitivity analysis in order to reduce the number of model parameters to be calibrated. Indeed, in the case of an over-parameterized model a sensitivity analysis may be performed in order to select the region in the space of input factors (i.e. parameters) on which to focus during the model calibration [36]. In this work, a preliminary screening of the most important kinetic, stoichiometric and fractionation model parameters by means of a preliminary GSA has been performed [37] replacing in the calibration protocol of the local approach with the global one [27]. In particular, the SRC method was employed.

The SRC method consists of running a Monte Carlo simulation (with random sampling of input factors i.e., the

parameters in our case) and performing a multivariate linear regression between the model output and the input factors. The SRC's (β_i), which represent the standardized regression slopes of the regression, are valid measures of sensitivity when, as suggested by Saltelli [36], the coefficient of determination R^2 is greater than 0.7. For linear models, $\sum(\beta_i)^2 = 1$ otherwise this sum is lower than 1 and represents the model coefficient of determination R^2 [38]. A high absolute value of β_i indicates a relevant effect of the related ith model parameter on the model output. The sign of β_i indicates its positive (sign +) or negative (sign −) influence on the model output [39].

After a preliminary trial and error calibration, the parameter values (of the important model parameters) have been estimated by applying a novel calibration protocol developed in a recent study [27]. In this calibration protocol, a step-wise Monte Carlo-based calibration is employed on the subset of important parameters. The main feature of this procedure is that different subsets of model parameters corresponding to sub-groups of model outputs are considered separately. In this way, the combination of issues related with the model complexity, the lack of data and the large number of parameters involved is tackled. The calibration protocol is based on the Generalized Likelihood Uncertainty Estimation (GLUE) methodology [40]. Such a methodology has the peculiarity to be based on the equifinality concept which considers that different parameter sets might provide acceptable model results when compared with the available observed data [41]. The GLUE does not require any particular additional assumptions (e.g. on correlation among parameters).

The calibration protocol simplifies the problem of finding the optimal parameter set by an iterative estimation approach. However, while the original form of the protocol uses a local sensitivity analysis, in this study a preliminary GSA is carried out in order to identify the most important model parameters to be calibrated for each model output sub-group. The sub-groups of model outputs and corresponding important parameters to be calibrated are then selected and the iterative step-wise procedure is applied considering a specific calibration order (defined either according to the modeler's experience or in an objective way considering a ranking order of the sensitivity sub-groups) of these output sub-groups.

In order to quantify how the variation of the important model parameters influences the model output (Y) and which set represents the best calibrated set, the expressions for the likelihood (Eq. 6) and global model efficiency (Eq. 7) used by Mannina et al. [27] were applied:

$$L(\theta_i/Y_j) = \exp\left(\frac{-\sigma^2_{Mj-Oj}}{\sigma^2_{Oj}}\right) \quad (6)$$

where θ_i, represents the ith set of (randomly generated) model parameters, $\sigma^2{}_{Mj-Oj}$ represents the sum of squared errors between model output (Mj, i) and observation (Oj, i) of the jth variable, while $\sigma^2{}_{Oj}$ is the sum of squared errors between the observations (Oj, i) and the average value of the observations $(\bar{O}_j)$ for the period under consideration.

$$E_i = \sum_j^n \alpha_j L(\theta_i/Y_j) \quad (7)$$

where E_i represents the weighted sum of the likelihood measures of the n model outputs computed on the ith selected parameter set (θ_i) and α_j is a normalizing constant that represents the weight of the jth model output.

The model as well as all the algorithms is coded in Fortran 95. Simulations were performed with an ASUS AMD Athlon 64 X2 Dual Core Processor 4000+, 2.1 GHz, with 2 GB RAM. One model simulation requires approximately 3 min.

Results and discussion

Preliminary sensitivity analysis

Twenty-one model output variables in four plant locations (locations 1, 2, 3 and 5 of Fig. 1) were taken into account. In particular, the following model output variables were considered: COD_{TOT}, S_{NH_4}, S_{NO_3}, S_{PO}, MLSS, for locations 1, 2, 3 and 5, COD_{SOL} (COD soluble) for location 3 and TN (total nitrogen) for location 5. The analysis has been performed considering all 79 model parameters.

The SRC method was applied considering the broadest variation range for each model parameter found in the relevant literature (among others, Vanrolleghem [42]; Brun et al. [21]; Hauduc et al. [43]) (Table 5). A parameter matrix (800 × 79) was generated using Latin hypercube sampling. Monte Carlo simulation was performed on the sampled parameter values. As in Sin et al. [39], abs(β_i) with values above 0.1 were selected as being important. For each of the 21 model output variables taken into account, the coefficient of determination R^2 was lower than 0.7, its value ranged from 0.23 to 0.51. Although the SRC method was applied outside its range of applicability ($R^2 < 0.7$). Cosenza et al. [37] have demonstrated that the ranking of important model parameters was very similar to the results obtained with the more reliable, but more demanding Extended-FAST GSA method. For each of the chosen pilot plant locations (i.e. locations 1, 2, 3 and 5 of Fig. 1) and for each of the 21 model output variables, a set of important model parameters has been selected by applying the SRC method. In particular, for each chosen plant location, the time-averaged output variables were

considered. Therefore, 79 sensitivity coefficients have been calculated for each of the 21 model output variables.

Globally, 24 model parameters (22 related to the biological sub-model and 2 related to the physical sub-model), having the $|\beta_i|$ value larger than 0.1, were classified as being important. A substantial reduction (>65 %) in the number of model parameters to calibrate was therefore accomplished. The model parameters classified as being important present good consistency with the relevant processes occurring in each plant location. For example, one of the most important parameters for $S_{PO,1}$ (orthophosphate in location 1) is q_{PHA} (rate constant for S_A uptake rate); this parameter is representative of the phosphorus release process which occurs in anaerobic conditions. The positive sign of the resulting value of β_i ($\beta_i = 0.32$) for q_{PHA} indicates a positive effect on $S_{PO,1}$. Another example is the influence of the parameters μ_H (maximum growth rate of heterotrophic organisms) and Y_H (yield coefficient for heterotrophic organisms growth) on the model output $S_{NO_3,2}$ with β_i, respectively, equal to -0.32 and 0.22. Moreover, the influence of parameter f (f represents the substrate fraction below the critical molecular weight able to be retained by the membrane) for COD sub-group represents the influence of the effect of physical separation. The negative value of β_i of parameter f for COD model outputs is in accordance with the physical interpretation; with increasing f a decrease in COD concentration takes place.

Table 4 summarizes the results of the sensitivity analysis for each sub-group of model outputs created in order to apply the calibration protocol. In particular, the MLSS, N, COD and P sub-groups of model outputs were considered; a model parameter is important for a sub-group if it is classified as important for at least one of the model outputs of that sub-group.

Only three model parameters (k_H, μ_H and f_{Xi}) have been considered important for the MLSS sub-group. The results related to the influence of f_{Xi} for MLSS are consistent with previous studies (i.e. Sin et al. [39] and Cheng et al. [44]) and have particular interest in the MBR context where accumulation of X_I occurs when operating with complete sludge retention.

Once the important model parameters have been selected, for each sub-group, the calibration order was defined (Table 4). For each selected model output, the sum of the absolute values of β_i for the important model parameters was computed first. Thereafter, the average sum of the β_i of each sub-group (β_M) has been calculated. The order of the different calibration sub-groups has been established by ranking the calibration sub-group with respect to β_M. The first calibration order has been assigned to the sub-group which presents the highest β_M value.

Calibration

Even though the calibration protocol does not specify a preliminary manual calibration, the computational time of the automatic calibration can be reduced by first performing a calibration by means of the trial and error method: according to the modeler's experience the default values (taken from literature) of some parameters are changed in order to improve the simulated versus measured concentration profiles of the model outputs taken into account. The a priori set of model parameters is thus obtained from this trial and error calibration (see values enclosed in parenthesis in the third column of Table 5). This set is equal to the default one except for the parameters f_{XI}, f_{BAP}, $i_{TSS,XI}$, $i_{TSS,XS}$, $i_{TSS,BM}$ and b_{AUT} which, respectively, represent the fraction of X_I generated in biomass decay, the fraction of BAP generated in biomass decay, the conversion factor X_I in TSS, the conversion factor X_S in TSS, the conversion factor biomass in TSS and the decay rate coefficient for autotrophic organisms. The parameters f_{XI} (default = 0.1, a priori = 0.05), f_{BAP} (default = 0.022, a priori = 0.007), $i_{TSS,XI}$ (default = 0.75, a priori = 0.7875), $i_{TSS,XS}$ (default = 0.75, a priori = 0.7875), $i_{TSS,BM}$ (default = 0.9, a priori = 0.945) were substantially changed in order to improve the fit between the simulated and measured MLSS values; the value of b_{AUT} (default = 0.15 day^{-1},

Table 4 Synthesis on the results of the preliminary sensitivity analysis: sub-groups of model outputs; model outputs taken into account during the analysis, calibration order, important model parameters for each sub-group and performed Monte Carlo (MC) runs for the model calibration

Sub-group	Model output	Calibration order	Important parameters sub-group	MC runs
P	$S_{PO,1}$, $S_{PO,2}$, $S_{PO,3}$, $S_{PO,5}$	I	k_H, η_{FE}, K_{NO_3}, μ_H, b_H, q_{PHA}, q_{PP}, μ_{PAO}, b_{PAO}, Y_H, f_{XI}, Y_{PAO}, $i_{P,XI}$, $i_{P,XS}$, $i_{P,BM}$	9,570
N	$S_{NH_4,1}$, $S_{NO_3,1}$, $S_{NH_4,2}$, $S_{NO_3,2}$, $S_{NH_4,3}$, $S_{NO_3,3}$, $TN_{,5}$, $S_{NH_4,5}$, $S_{NO_3,5}$	II	k_H, K_O, μ_H, $\eta_{NO_3,H}$, b_H, $K_{NH,H}$, μ_{AUT}, Y_H, f_{XI}, F_{SA}, f, $i_{N,XI}$, $i_{N,XS}$	3,444
COD	$COD_{TOT,1}$, $COD_{TOT,2}$, $COD_{TOT,3}$, $COD_{SOL,3}$, $COD_{TOT,5}$	III	k_H, μ_H, b_H, $K_{NH,H}$, μ_{AUT}, Y_H, β, f	3,379
MLSS	MLSS,1, MLSS,2, MLSS,3	IV	k_H, μ_H, f_{XI}	3,502

Table 5 Values of model parameters (default, a priori and calibrated), variation ranges and literature references; the value enclosed in parenthesis is the a priori value

Symbol	Unit	Default	Min	Max	Calibrated	References
k_H	g X_Sg X_H^{-1} day^{-1}	3	1.5	4.5	1.7248	[21]
$\eta_{NO_3,HYD}$	–	0.6	0.402	0.798	–	[43]
η_{FE}	–	0.4	0.2	0.6	0.4786	[43]
K_O	g S_{O_2} m^{-3}	0.2	0.1	1	0.5388	[42]
K_{NO3}	g S_{NO_3} m^{-3}	0.5	0.1	0.625	0.3157	[21, 42]
K_X	g X_S g X_H^{-1}	0.1	0.05	0.15	–	[21]
$K_{O,HYD}$	g S_{O_2} m^{-3}	0.2	0.1	0.3	–	[21]
$K_{NO_3,HYD}$	g N m^{-3}	0.5	0.375	0.625	–	[21]
μ_H	day^{-1}	6	0.6	13.2	1.3000	[46]
q_{FE}	g S_F g X_H^{-1} day^{-1}	3	1.5	4.5	–	[21]
$\eta_{NO_3,HYD}$	–	0.8	0.6	1	0.9852	[21]
b_H	day^{-1}	0.4	0.05	1.6	0.5829	[46]
K_F	g S_F m^{-3}	4	2	6	–	[21]
K_{FE}	g S_F m^{-3}	4	2	6	–	[21]
K_A	g S_A m^{-3}	4	2	6	–	[21]
$K_{NH,H}$	g S_{NH_4} m^{-3}	0.05	0.02	2	0.0953	[42]
K_P	g S_{PO_4} m^{-3}	0.01	0.005	0.015	–	[21]
$K_{ALK,H}$	mol HCO_3^- m^{-3}	0.1	0.05	0.15	–	[21]
q_{PHA}	g X_{PHA} g X_{PAO}^{-1} day^{-1}	3	0.3	5.7	3.6991	[43]
q_{PP}	g X_{PP} g X_{PAO}^{-1} day^{-1}	1.5	0	3.3	2.3413	[43]
μ_{PAO}	day^{-1}	1	0.5	1.5	0.7167	[21]
$\eta_{NO_3,PAO}$	–	0.6	0.45	0.75	–	[21]
b_{PAO}	day^{-1}	0.2	0.1	0.25	0.2351	[32, 43]
b_{PP}	day^{-1}	0.2	0.1	0.25	–	[32, 43]
b_{PHA}	day^{-1}	0.2	0.1	0.25	–	[32, 43]
K_{PS}	g S_{PO_4} m^{-3}	0.2	0.1	0.3	–	[21]
K_{PP}	g X_{PP} g X_{PAO}^{-1}	0.01	0.005	0.015	–	[21]
K_{max}	g X_{PP} g X_{PAO}^{-1}	0.34	0.2	0.51	–	[47]
K_{IPP}	g X_{PP} g X_{PAO}^{-1}	0.02	0.01	0.03	–	[21]
K_{PHA}	g X_{PHA} g X_{PAO}^{-1}	0.01	0.005	0.015	–	[21]
$K_{O,PAO}$	g S_{O_2} m^{-3}	0.2	0.1	0.3	–	[21]
$K_{NO_3,PAO}$	g S_{NO_3} m^{-3}	0.5	0.375	0.625	–	[21]
$K_{A,PAO}$	g S_A m^{-3}	4	2	6	–	[21]
$K_{NH,PAO}$	g S_{NH_4} m^{-3}	0.05	0.025	0.075	–	[21]
$K_{P,PAO}$	g S_{PO_4} m^{-3}	0.01	0.005	0.015	–	[21]
$K_{ALK,PAO}$	mol HCO_3^- m^{-3}	0.1	0.05	0.15	–	[21]
μ_{AUT}	day^{-1}	1	0.2	1.2	1.1810	[42]
b_{AUT}	day^{-1}	0.15 (0.08)	0.04	0.1605	–	[43]
$K_{O,A}$	g S_{O_2} m^{-3}	0.5	0.1	2	–	[42, 46]
$K_{NH,A}$	g S_{NH_4} m^{-3}	1	0.5	1.5	–	[43]
$K_{ALK,A}$	mol HCO_3^- m^{-3}	0.5	0.25	0.75	–	[21]
$K_{P,A}$	g S_{PO_4} m^{-3}	0.01	0.005	0.015	–	[21]
$k_{H,BAP}$	day^{-1}	0.000000741	3.705E−07	1.1115E−06	–	[9]
$k_{H,UAP}$	day^{-1}	0.0102	0.0051	0.0153	–	[9]
$k_{LaT,3}$	h^{-1}	10	9.5	10.5	–	[48]
$k_{LaT,4}$	h^{-1}	3.4	3.23	3.57	–	[48]
Y_H	g X_H g X_S^{-1}	0.625	0.38	0.75	0.3913	[46]

Table 5 continued

Symbol	Unit	Default	Min	Max	Calibrated	References
f_{XI}	g X_I g X_H^{-1}	0.1 (0.05)	0.05	0.4	0.0600	[42]
Y_{PAO}	g X_{PAO} g X_{PHA}^{-1}	0.625	0.42	0.78125	0.4428	[21]
Y_{PO_4}		0.4	0.38	0.42	–	[21]
Y_{PHA}	g X_{PP} g X_{PHA}^{-1}	0.2	0.19	0.21	–	[21]
Y_A	g X_{PP} g X_{PHA}^{-1}	0.24	0.228	0.252	–	[21]
f_{BAP}	–	0.0215 (0.007)	0.0069	0.022575	–	[21]
f_{UAP}	–	0.0963	0.091485	0.101115	–	[21]
F_{SF}	–	0.12	0.06	0.18	–	[21]
F_{SA}	–	0.08	0.04	0.12	0.0425	[21]
F_{SI}	–	0.12	0.114	0.126	–	[21]
F_{XI}	–	0.1	0.05	0.15	–	[21]
F_{XH}	–	0.1	0.06	0.18	–	[21]
β	–	0.01234509	1.00E−04	2.10E−02	0.0138	[16]
α	–	0.47773695	0	1	–	[16]
γ	kg m^{-3} s	0.00242427	5.56E−04	2.78E−03	–	[16]
F	–	0.18	0.001	0.99	0.9104	[16]
λ	m^{-1}	1,520.291091	1,000	2.00E + 03	–	[16]
C_E	–	0.99794265	0.996	0.999	–	[16]
$i_{N,SI}$	g N g S_I^{-1}	0.01	0.0075	0.0125	–	[21]
$i_{N,SF}$	g N g S_F^{-1}	0.03	0.0225	0.0375	–	[21]
$i_{N,XI}$	g N g X_I^{-1}	0.02	0.015	0.025	0.0245	[21]
$i_{N,XS}$	g N g X_S^{-1}	0.04	0.03	0.05	0.0437	[21]
$i_{N,BM}$	g N g X_{BM}^{-1}	0.07	0.0665	0.0735	–	[21]
$i_{P,SF}$	g P g S_F^{-1}	0.01	0.005	0.015	–	[21]
$i_{P,XI}$	g P g X_I^{-1}	0.01	0.005	0.015	0.0056	[21]
$i_{P,XS}$	g P g X_S^{-1}	0.01	0.005	0.015	0.0099	[21]
$i_{P,BM}$	g P g X_{BM}^{-1}	0.02	0.015	0.025	0.0207	[21]
$i_{TSS,XI}$	g TSS g X_I^{-1}	0.75 (0.7875)	0.7125	0.7875	–	[21]
$i_{TSS,XS}$	g TSS g X_S^{-1}	0.75 (0.7875)	0.7125	0.7875	–	[21]
$i_{TSS,BM}$	g TSS g X_{BM}^{-1}	0.9 (0.945)	0.855	0.945	–	[21]
$i_{TSS,XPHA}$	g TSS g X_{PHA}^{-1}	0.6	0.57	0.63	–	[21]
$i_{TSS,XPP}$	g TSS g X_{PP}^{-1}	3.23	3.0685	3.3915	–	[21]

a priori = 0.08 day^{-1}) was reduced in order to improve the description of the nitrification process. The b_{AUT} value is in agreement with values found in literature for MBR systems [4, 28]. After trial and error calibration, the efficiency of each model output related to the a priori parameter value, $E_{a\ priori}(i)$, and the global model efficiency, computed according to Eq. 7, have been evaluated. A global model efficiency equal to 0.29 was obtained. However, the model output variables total COD and S_{NO_3} for each plant location, S_{PO} for the locations 3 and 5 and $TN_{,5}$ still presented very low efficiency values.

Then, the important model parameters of Table 4 were calibrated by applying the calibration protocol proposed by Mannina et al. [27] considering the model outputs of Table 4.

For each sub-group, starting from the first sub-group (P) up till the last one (MLSS), several Monte Carlo runs (Table 4) were performed, each time varying only the important parameters for this sub-group (non important model parameters are maintained equal to their a priori value). The required number of MC runs (Table 4) was different from sub-group to sub-group. Similarly to Mannina et al. [27], this study was carried out by analyzing the model efficiency variations while increasing the sample dimension from 100 to 10,000 Monte Carlo simulations. The same parameter ranges as used in the preliminary sensitivity analysis were used (Table 5) and no a priori correlation between parameters was assumed.

For each run, simulated outputs were compared with measured data computing the model output efficiency according to Eq. 6. For each sub-group, the calibrated set

Table 6 Values of the $E_{a\ priori}$, E_{max}, respectively, for each model output i and $E_{SUB\text{-}GROUP}$, E_{MOD} and number of observed data

Variable (i)	No. data	$E_{a\ priori}$(i)	1° step sub-group P E_{max}(i)	2° step sub-group N E_{max}(i)	3° step sub-group COD E_{max}(i)	4° step sub-group MLSS E_{max}(i)
$COD_{TOT,1}$	50	0.00	0.01	0.01	0.12	0.13
$S_{NO_3,1}$	50	0.09	0.14	0.14	0.14	0.16
$S_{NH_4,1}$	34	0.35	0.34	0.35	0.35	0.36
$S_{PO,1}$	53	0.36	0.51	0.50	0.50	0.53
$MLSS_{,1}$	59	0.08	0.05	0.05	0.15	0.37
$COD_{TOT,2}$	46	0.01	0.01	0.01	0.16	0.26
$S_{NH_4,2}$	21	0.16	0.17	0.17	0.17	0.18
$S_{NO_3,2}$	53	0.00	0.03	0.16	0.16	0.16
$S_{PO,2}$	45	0.47	0.62	0.62	0.62	0.63
$MLSS_{,2}$	57	0.19	0.01	0.01	0.11	0.36
$COD_{TOT,3}$	49	0.00	0.00	0.00	0.19	0.20
$COD_{SOL,3}$	43	0.25	0.16	0.02	0.24	0.27
$S_{NH_4,3}$	44	0.25	0.23	0.27	0.27	0.27
$S_{NO_3,3}$	27	0.00	0.00	0.00	0.15	0.16
$S_{PO,3}$	52	0.00	0.10	0.11	0.12	0.12
$MLSS_{,3}$	58	0.12	0.03	0.03	0.13	0.30
$COD_{TOT,5}$	22	0.08	0.12	0.13	0.18	0.20
$S_{NH_4,5}$	39	0.20	0.19	0.27	0.27	0.28
$S_{NO_3,5}$	37	0.01	0.01	0.01	0.15	0.16
$TN_{,5}$	40	0.00	0.00	0.19	0.18	0.19
$S_{PO,5}$	50	0.00	0.10	0.12	0.12	0.12
$E_{SUB\text{-}GROUP}$	–	–	0.50	0.36	0.29	0.39
E_{MOD}	–	0.28	0.33	0.34	0.35	0.39

of parameters, corresponding to the maximum value of the global model efficiency ($E_{max,i}$ computed by using Eq. 7) was selected. Moreover, for each step the efficiency related to the sub-group ($E_{SUB\text{-}GROUP}$) under study was computed, according to Eq. 7, considering only the model outputs of that sub-group. In contrast, the global model efficiency (E_{MOD}) considers the model outputs of the sub-group under study and all previous sub-groups in the calibration order. Table 6 summarizes results related to each calibration phase (including trial and error) in terms of model output efficiency, global model efficiency and the number of observed data. Important to note is that, according to the adopted criteria for model parameter estimation, the efficiencies related to the fourth step represent the final value for the calibrated model. In Table 6, the step-by-step increase of E_{max} and consequently of $E_{SUB\text{-}GROUP}$ and E_{MOD} can be observed. The greatest increase of the E_{max} value, compared to its a priori value, was obtained for $MLSS_{,1}$ and $COD_{TOT,2}$. The efficiency values for $MLSS_{,1}$ and $COD_{TOT,2}$ increased, respectively, by 29 and 25 % of the a priori value. High final values of E_{max} were obtained for $S_{PO,1}$ and $S_{PO,2}$ (0.53 and 0.63, respectively, see Table 6) demonstrating a good ability of the model to describe the anaerobic phosphorus release. However, low values of E_{max} were obtained for $S_{PO,3}$ and $S_{PO,5}$ (both equal to 0.12). This result might be due to the un-modeled release of phosphorus due to the possible anaerobic conditions occurring inside the cake layer formed on the membrane surface, as experimentally demonstrated by Fu et al. [7].

The calibrated parameter values are summarized in Table 5. Most of them are in agreement with literature values (among others, Henze et al. [32]; Jiang et al. [9]; Fenu et al. [8]; Hauduc et al. [43]). However, some values of the calibrated model parameters require further discussion. The calibrated value of μ_{AUT} (1.18 day^{-1}) is different from the value presented by Jiang [45] who, applying the ASM2d-SMP model, obtained a value equal to 0.6 day^{-1}. The calibrated values of Y_H and b_H, respectively, equal to 0.39 gX_H/gX_S and 0.58 day^{-1}, correspond with values obtained independently by means of respirometry [4].

The calibrated value of q_{pp} (2.34 $gX_{PP}\ gX_{PAO}^{-1}\ day^{-1}$) is considerably higher than the value obtained by Jiang [45] ($q_{pp} = 1.1\ gX_{PP}\ gX_{PAO}^{-1}\ day^{-1}$). This parameter value describes the storage process of poly-phosphate that in the analyzed plant was higher. Indeed, the orthophosphate

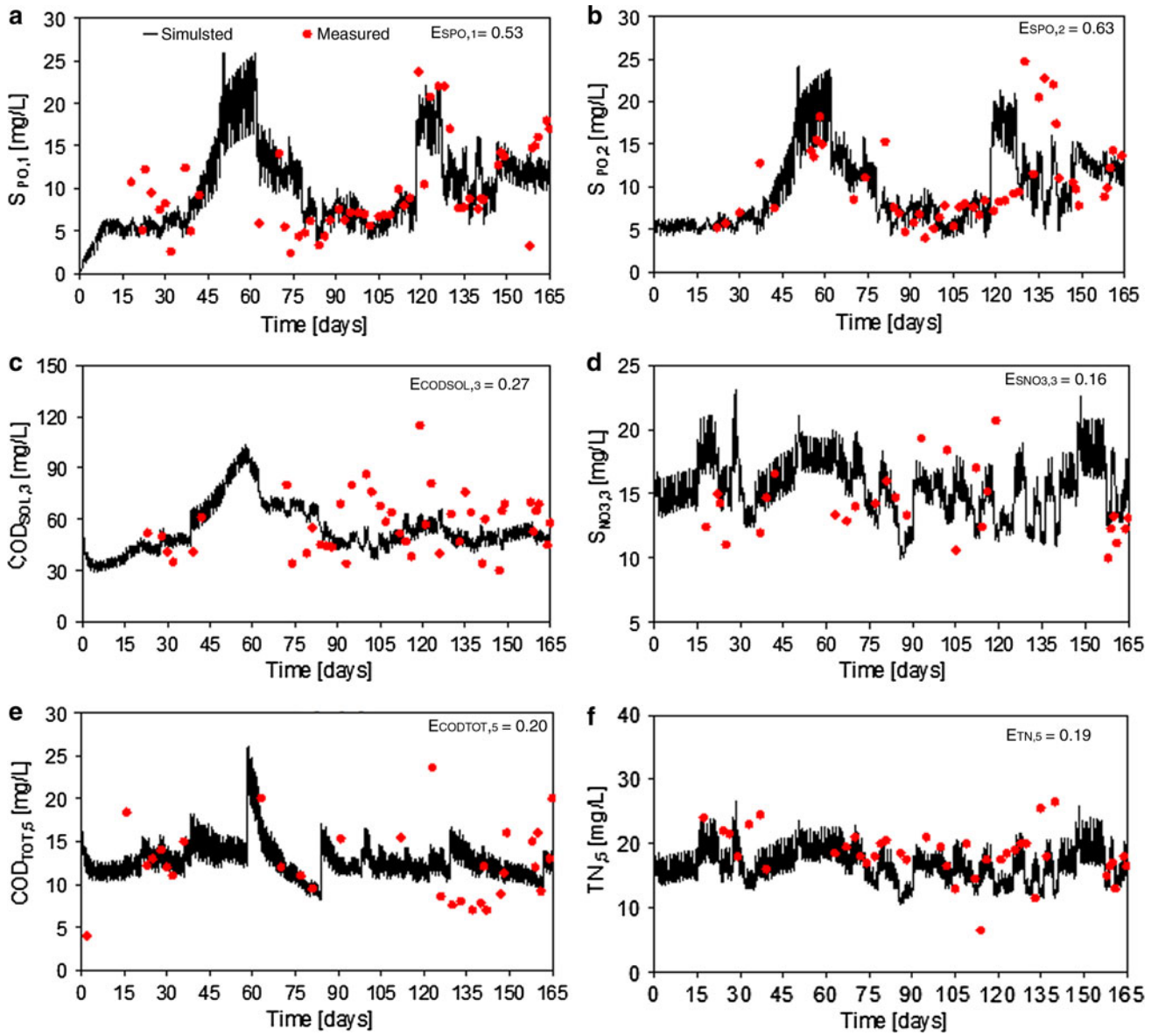

Fig. 2 Simulated versus measured values for orthophosphate and mixed liquor suspended solids in the anaerobic and anoxic tanks, respectively, $S_{PO,1}$ (**a**), $S_{PO,2}$ (**b**), total soluble COD and nitrate in the aerobic tank, respectively, $COD_{SOL,3}$ (**c**), $S_{NO_3,3}$ (**d**) and total COD and nitrogen in the permeate, respectively, $COD_{TOT,5}$ (**e**), TN_5 (**f**)

assimilation took place not only in the aerobic tank but also in the anoxic one. Furthermore, this parameter takes into account the increasing storage rate during the period of K_2PO_4 dosing.

The model calibration results showed an acceptable correspondence with experimental data (final model efficiency equal to 0.39). The satisfactory responses of the calibrated model demonstrate the ability of the adopted calibration procedure to be used also for very complex models, by taking into account the results of a global instead of a local sensitivity analysis as considered in the original form of the protocol [27].

In Fig. 2, for example, a good prediction accuracy with respect to the long-term behaviour of some model outputs and related efficiencies ($E_{SPO,1}$, $E_{SPO,2}$, $E_{CODSOL,3}$, $E_{SNO_3,3}$, $E_{CODTOT,5}$, $E_{TN,5}$, $E_{MLSS,1}$, $E_{MLSS,2}$ and $E_{MLSS,3}$) are observed.

Important to note is that the model is able to reproduce the effect, in terms of $S_{PO,1}$ and $S_{PO,2}$ concentration (Fig. 2a, b), of the influent KH_2PO_4 dosing (performed from day 119 to 126 in order to increase the influent P-PO_4 concentration). The ability of the model to reproduce the nitrification and denitrification processes in the aerobic and anaerobic tank is represented in Fig. 2f, h.

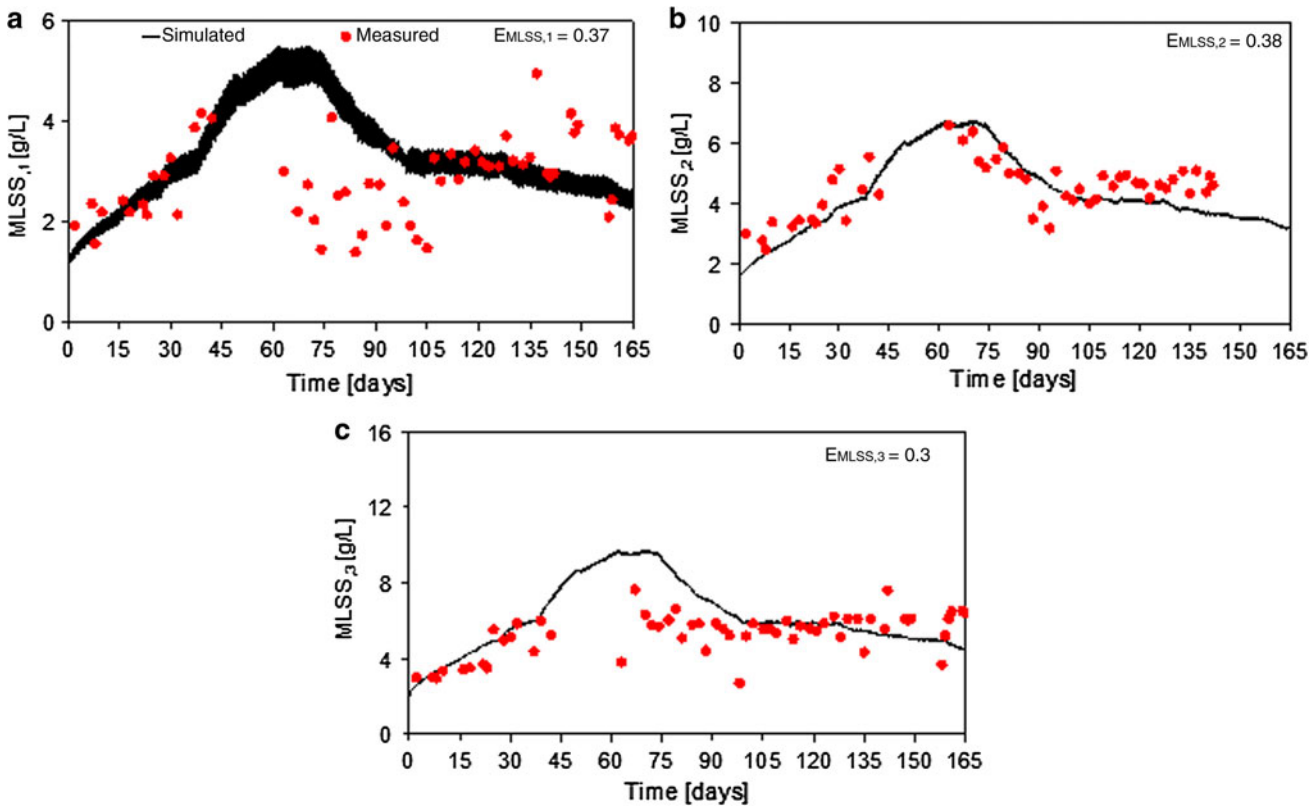

Fig. 3 Simulated versus measured values for $MLSS_{,1}$ (**a**), $MLSS_{,2}$ (**b**) and $MLSS_{,3}$ (**c**)

Regarding the $COD_{TOT,5}$, the good agreement between observed and simulated values is shown in Fig. 2e, with the exception of the last period; the model is also able to reproduce the effect of the physical or chemical membrane cleaning (see the discontinuity around day 60 in Fig. 2e). Important to note is that a substantial difference between simulated values of $COD_{SOL,3}$ and $COD_{TOT,5}$ (Fig. 2c, e) occurs. This substantial difference is due to the ability of the model to simulate the contribution on the COD removal of the dynamic membrane.

In terms of MLSS concentration the model over-predicts the simulated values from day 45 to day 90 in the anaerobic tank (Fig. 3a). The authors associate such result to the model's incapacity to reproduce the stress condition imposed on the biomass by the frequent energy interruption in the pilot plant from day 45 to day 90. Due to this interruption, the feeding valve stayed open causing the washout of the biomass from the anaerobic to the anoxic tank. Obviously such plant malfunction affects the measured MLSS concentration more in the anaerobic tank than the anoxic one, the latter being protected by the high solid concentration of Q_{R2} mixed liquor recycle. Indeed, much better fitting between measured and simulated data of $MLSS_{,2}$ and $MLSS_{,3}$ are shown, respectively, in Fig. 3b, c.

Even though S_{UAP} and S_{BAP} were not used in the calibration process, because no consistent data were available, the modeled values of S_{UAP} and S_{BAP} (Fig. 4) are consistent with Jiang [45]. Indeed, an increase of SRT, due to the complete sludge retention in the first period, generates an increase in S_{UAP} until the beginning of sludge withdrawal. It is also important to mention that the S_{UAP} concentration peak (around 60 mg L^{-1}) occurred at the same time as the inflow of water with a high influent soluble COD concentration (around 200 mg L^{-1}) (Fig. 4).

Globally, the best fit between simulated and measured data in terms of efficiency was obtained for $S_{PO,1}$ and $S_{PO,2}$ with efficiency values of 0.52 and 0.63, respectively. The global model efficiency after applying the calibration protocol was equal to 0.39 (computed as weighted sum over all 21 variables taken into account). This value has considerably increased compared to the value of 0.1 obtained by using the default values of the parameters suggested in literature. However, the results have undoubtedly been influenced by the data quality. Nevertheless, the model response may be considered acceptable in view of the complexity of the analyzed system. Indeed the results are conditioned to a large number of model outputs (21).

It is important to specify that in this study the attention lies only on the selection of important parameters and on their estimation without performing any specific investigation in terms of identifiability (among others, Brun et al.

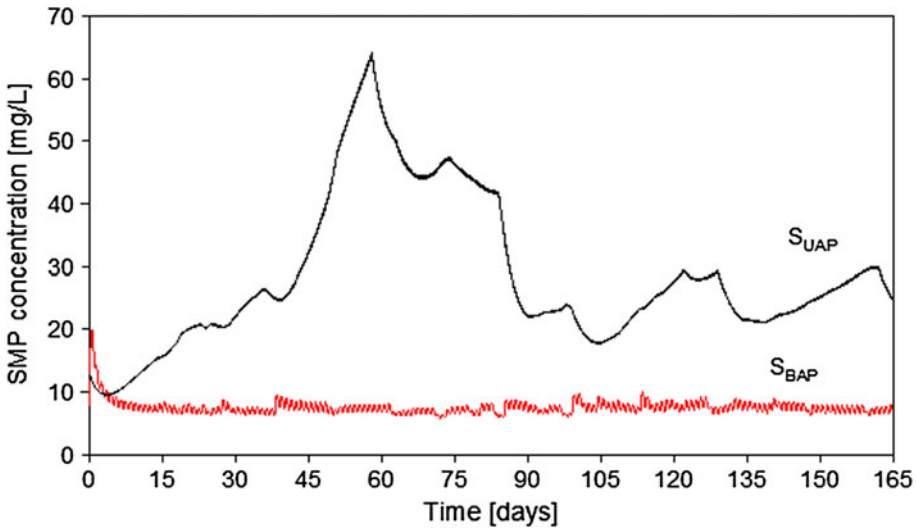

Fig. 4 Simulated S_{UAP} and S_{BAP} profiles in the aerobic tank

[21]). The identifiability analysis was out of the scope of the present study.

Conclusions

An integrated mathematical model able to describe the BNR processes and the cake layer contribution to the COD removal was presented. The key points of the model are:

- The biological sub-model was developed by extending the ASM2d-SMP model of Jiang et al. [9] by introducing the hydrolysis process of X_I as suggested by Lubello et al. [31].
- The physical sub-model is able to describe the mechanisms for attachment and detachment biomass on the membrane surface and the thickness of the cake layer.
- The integrated model is able to describe the global membrane (physical and biological) contribution to COD_{TOT} removal.

The model was calibrated by using a modified version of a novel calibration protocol, proposed by Mannina et al. [27]. In particular, the local sensitivity analysis was replaced by the GSA for the identification of the most important model parameters. By performing the GSA for the case study 24 important model parameters were selected, substantially reducing (>65 %) the number of model parameters to calibrate. Despite the model complexity, the protocol provided acceptable results by applying a GSA, rarely used in the field of wastewater models, for the important parameters screening. The simulated values of S_{UAP} and S_{BAP} were not used to calibrate the model due to a lack of measured values. However, the modeled concentrations of SMP were consistent with the reversible membrane fouling noticed during the pilot plant operation. The integrated model represents a useful tool to improve MBR plant design and to pre-emptively evaluate the SMP concentration in an MBR system.

Acknowledgments Peter Vanrolleghem holds the Canada Research Chair in Water Quality Modelling.

References

1. Trussell RS, Merlo RP, Hermanowicz SW, Jenkins D (2006) The effect of organic loading on process performance and membrane fouling in a submerged membrane bioreactor treating municipal wastewater. Water Res 40(14):2675–2683
2. Judd SJ, Judd C (2010) Principles and applications of membrane bioreactors in water and wastewater treatment, 2nd edn. Elsevier, London
3. Jiang T, Sin G, Spanjers H, Nopens I, Kennedy M, van der Meer W, Futselaar H, Amy G, Vanrolleghem PA (2009) Comparison of the modeling approach between membrane bioreactor and conventional activated sludge processes. Water Environ Res 81(4):432–440
4. Di Trapani D, Capodici M, Cosenza A, Di Bella G, Mannina G, Torregrossa M, Viviani G (2011) Evaluation of biomass activity and wastewater characterization in a UCT-MBR pilot plant by means of respirometric techniques. Desalination 269:190–197
5. Le-Clech P, Chen V, Fane TAG (2006) Fouling in membrane bioreactors used in wastewater treatment. J Membr Sci 284(1–2):17–53
6. Meng F, Chae SR, Drews A, Kraume M, Shin HS, Yang F (2009) Recent advances in membrane bioreactors (MBRs): membrane fouling and membrane material. Water Res 43:1489–1512
7. Drews A (2010) Membrane fouling in membrane bioreactors—characterisation, contradictions, cause and cures. J Membr Sci 363(1–2):1–28
8. Fenu A, Guglielmi G, Jimenez J, Spèrandio M, Saroj D, Lesjean B, Brepols C, Thoeye C, Nopens I (2010) Activated sludge model (ASM) based modelling of membrane bioreactor (MBR) processes: a critical review with special regard to MBR specificities. Water Res 44(15):4272–4294
9. Jiang T, Myngheer S, De Pauw DJW, Spanjers H, Nopens I, Kennedy MD, Amy G, Vanrolleghem PA (2008) Modelling the production and degradation of soluble microbial products (SMP) in membrane bioreactors (MBR). Water Res 42(20):4955–4964

10. Spérandio M, Espinosa MC (2008) Modelling an aerobic submerged membrane bioreactor with ASM models on a large range of sludge retention time. Desalination 231(1–3):82–90
11. Mannina G, Di Bella G, Viviani G (2010) Uncertainty assessment of a membrane bioreactor model using the GLUE methodology. Biochem Eng J 52(2):263–275
12. Ahmed Z, Cho J, Lim BR, Song KG, Ahn KH (2007) Effects of sludge retention time on membrane fouling and microbial community structure in a membrane bioreactor. J Membr Sci 287:211–218
13. Ng HY, Kim AS (2007) A mini-review of modelling studies on membrane bioreactor (MBR) treatment for municipal wastewaters. Desalination 212:261–281
14. Zarragoitia-González A, Schetrite S, Alliet M, Jáuregui-Haza U, Albasi C (2008) Modelling of submerged membrane bioreactor: conceptual study about link between activated sludge biokinetics, aeration and fouling process. J Membr Sci 325:612–624
15. Lu SG, Imai T, Ukita M, Sekine M, Higuchi T, Fukagawa M (2001) A model for membrane bioreactor process based on the concept of formation and degradation of soluble microbial products. Water Res 35(8):2038–2048
16. Di Bella G, Mannina G, Viviani G (2008) An integrated model for physical-biological wastewater organic removal in a submerged membrane bioreactor: model development and parameter estimation. J Membr Sci 322(1):1–12
17. Kuberkar VT, Davis RH (2000) Modeling of fouling reduction by secondary membranes. J Membr Sci 168:243–257
18. Mannina G, Di Bella G, Viviani G (2011) An integrated model for biological and physical process simulation in membrane bioreactors (MBRs). J Membr Sci 376:56–69
19. Zuthi MFR, Ngo HH, Guo WS (2012) Modelling bioprocesses and membrane fouling in membrane bioreactor (MBR): a review towards finding an integrated model framework. Bioresour Technol (in press)
20. Naessens W, Maere T, Nopens I (2012) Critical review of membrane bioreactor models-Part 1: biokinetic and filtration models. Bioresour Technol (in press)
21. Brun R, Kühni M, Siegrist H, Gujer W, Reichert P (2002) Practical identifiability of ASM2d parameters-systematic selection and tuning of parameter subsets. Water Res 36:4113–4127
22. Hulsbeek JJW, Kruit J, Roeleveld PJ, van Loosdrecht MCM (2002) A practical protocol for dynamic modelling of activated sludge systems. Water Sci Technol 45(6):127–136
23. Petersen B, Gernaey K, Henze M, Vanrolleghem PA (2002) Evaluation of an ASM1 model calibration procedure on a municipal-industrial wastewater treatment plant. J Hydroinform 4(1):15–38
24. Vanrolleghem PA, Insel G, Petersen B, Sin G, De Pauw D, Nopens I, Weijers S, Gernaey K (2003) A comprehensive model calibration procedure for activated sludge models. In: Proceedings of the 76th annual WEF technical exhibition and conference (WEFTEC2003), Los Angeles, USA, October 11–15
25. Melcer H, Dold PL, Jones RM, Bye CM, Takacs I, Stensel HD, Wilson AW, Sun P, Bury S (2003) Methods for wastewater characterization in activated sludge modeling. Water Environment Research Foundation (WERF), Alexandria
26. Langergraber G, Rieger L, Winkler S, Alex J, Wiese J, Owerdieck C, Ahnert M, Simon J, Maurer M (2004) A guideline for simulation studies of wastewater treatment plants. Water Sci Technol 50(7):131–138
27. Mannina G, Cosenza A, Vanrolleghem PA, Viviani G (2011) A practical protocol for calibration of nutrient removal wastewater treatment models. J Hydroinform 13:575–595
28. Saltelli A, Tarantola S, Chan KPS (1999) A quantitative model-independent method for global sensitivity analysis of model output. Technometrics 41(1):39–56
29. Neumann MB, Gujer W, von Gunten U (2009) Global sensitivity analysis for model-based prediction of oxidative micropollutant transformation during drinking water treatment. Water Res 43:997–1004
30. Hauduc H, Gillot S, Rieger L, Ohtsuki T, Shaw A, Takács I, Winkler S (2009) Activated sludge modelling in practice: an international survey. Water Sci Technol 60(8):1943–1951
31. Lubello C, Caffaz S, Gori R, Munz G (2009) A modified activated sludge model to estimate solids production at low and high solids retention time. Water Res 43(18):4539–4548
32. Henze M, Gujer W, Mino T, van Loosdrecht MCM (2000) Activated sludge models ASM1, ASM2, ASM2d and ASM3. IWA task group on mathematical modelling for design and operation of biological wastewater treatment. IWA Publishing, London
33. Li X, Wang X (2006) Modelling of membrane fouling in a submerged membrane bioreactor. J Membr Sci 278:151–161
34. Jang N, Ren X, Cho J, Kim IS (2006) Steady-state modelling of biofouling potentials with respect to the biological kinetics in the submerged membrane bioreactor. J Membr Sci 284:352–360
35. APHA, AWWA, WEF (1998) Standard methods for the examination of water and wastewater, 20th edn. American Public Health Association/American Water Works Association/Water Environment Federation, Washington, DC, USA
36. Saltelli A, Tarantola S, Campolongo F, Ratto M (2004) Sensitivity analysis in practice: a guide to assessing scientific models. John Wiley & Sons, Ltd, Chichester
37. Cosenza A, Mannina G, Neumann MB, Vanrolleghem PA, Viviani G (2011) Global sensitivity analysis in ASM applications: comparison of different methods. In: Proceedings of watermatex 2011, 8th IWA symposium on systems analysis and integrated assessment. San Sebastiàn, Spain, June 20–22, 2011
38. Saltelli A, Ratto M, Andres T, Campolongo F, Cariboni J, Gatelli D, Saisana M, Tarantola S (2008) Global sensitivity analysis. The Primer. John Wiley & Sons Ltd, The Atrium, Southern Gate, Chichester
39. Sin G, Gernaey KV, Neumann MB, van Loosdrecht MCM, Gujer W (2011) Global sensitivity analysis in wastewater treatment plant model applications: prioritizing sources of uncertainty. Water Res 45:639–651
40. Beven KJ, Binley A (1992) The future of distributed models: model calibration and uncertainty prediction. Hydrolog Processes 6(3):279–298
41. Beven KJ (2006) A manifesto for the equifinality thesis. J Hydrol 320(1–2):18–36
42. Weijers SR, Vanrolleghem PA (1997) A procedure for selecting best identifiable parameters in calibrating activated sludge model No.1 to full-scale plant data. Water Sci Technol 36(5):69–79
43. Hauduc H, Rieger L, Ohtsuki T, Shaw A, Takács I, Winkler S, Héduit A, Vanrolleghem PA, Gillot S (2011) Activated sludge modelling: development and potential use of a practical applications database. Water Sci Technol 63(10):2164–2182
44. Cheng L, Tian Y, Cao C, Zhang S, Zhang S (2012) Sensitivity and uncertainty analyses of an extended ASM3-SMP model describing membrane bioreactor operation. J Membr Sci 389:99–109
45. Jiang T (2007) Characterization and modelling of soluble microbial products in membrane bioreactors. PhD thesis, Ghent University, Belgium
46. Jeppsson U (1996) Modelling aspect of wastewater treatment process. PhD thesis, Department of Industrial Electrical Engineering and Automation (IEA), Lund Institute of Technology (LTH), Sweden
47. Rieger L, Koch G, Kühni M, Gujer W, Siegrist H (2001) The EAWAG Bio-P module for activated sludge model No. 3. Water Res 35(16):3887–3903
48. Innocenti V (2005) Modello di depurazione biologica secondo lo standard ASM3 con doppio step di nitrificazione. Degree thesis, Università degli Studi di Firenze, Italy (in Italian)